Molecular Cell *23*, 343–354, August 4, 2006 ©2006 Elsevier Inc. DOI 10.1016/j.molcel.2006.06.015

Structural Basis for Specificity in the Poxvirus Topoisomerase

Kay Perry,[1] Young Hwang,[2] Frederic D. Bushman,[2,*] and Gregory D. Van Duyne[1,*]
[1] University of Pennsylvania School of Medicine
Department of Biochemistry and Biophysics and
Howard Hughes Medical Institute
242 Anatomy-Chemistry Building
[2] University of Pennsylvania School of Medicine
Department of Microbiology
3610 Hamilton Walk
Philadelphia, Pennsylvania 19104

Summary

Although smallpox has been eradicated from the human population, it is presently feared as a possible agent of bioterrorism. The smallpox virus codes for its own topoisomerase enzyme that differs from its cellular counterpart by requiring a specific DNA sequence for activation of catalysis. Here we present crystal structures of the smallpox virus topoisomerase enzyme bound both covalently and noncovalently to a specific DNA sequence. These structures reveal the basis for site-specific DNA recognition, and they explain how catalysis is likely activated by formation of a specific enzyme-DNA interface. Unexpectedly, the poxvirus enzyme uses a major groove binding α helix that is not present in the human enzyme to recognize part of the core recognition sequence and activate the enzyme for catalysis. The topoisomerase-DNA complex structures also provide a three-dimensional framework that may facilitate the rational design of therapeutic agents to treat poxvirus infections.

Introduction

Smallpox is caused by the *variola* virus, a member of the Poxviridae virus family. The virus is highly transmissible with infection typically resulting in 20%–30% mortality, making it one of the most severe infectious diseases known to humans. The efficiency with which it spreads, combined with the deadly nature of the disease, has raised fears that smallpox could be revived for use in bioterrorism (Harrison et al., 2004). Structural models of smallpox virus proteins could provide the basis for rational design of antiviral agents, but few high-resolution structures of intact proteins from *variola* or related viruses have so far been reported (Moss, 2001).

Poxviruses are large, double-stranded DNA viruses that carry out their replication cycles entirely in the cytoplasm of infected cells. These viruses consequently encode many of the enzymes required to replicate and transcribe their genomes. Among these is a type IB topoisomerase, which is required for efficient transcription of the viral DNA (Da Fonseca and Moss, 2003). Type IB topoisomerase (TopIB) enzymes introduce transient breaks in one of the two strands of duplex DNA, allowing rotation of the flanking duplexes about the uncleaved strand (Figure 1A). These enzymes play critical roles in processes such as transcription, replication, and repair by relieving the topological stress caused by underwinding or overwinding of the DNA double helix that occurs during these events (Shuman, 1998; Wang, 1996).

The highly conserved poxvirus TopIBs are unique in several respects. They are among the smallest topoisomerases known, at only 34 kDa. Unlike the related eukaryotic cellular TopIB, which exhibits only a weak preference for certain DNA sequences (Been et al., 1984), the viral enzymes relax their substrates at specific DNA sites containing the core pentamer, 5′-(T/C)CCTT-3′ (Hwang et al., 1998; Shuman and Prescott, 1990). Since topoisomerase activity requires the presence of the proper recognition sequence (Hwang et al., 1999a; Shuman and Prescott, 1990; Tian et al., 2004; Wittschieben and Shuman, 1997), this raises important mechanistic questions about how catalysis is coupled to sequence-specific recognition in the poxvirus enzymes. Extensive biochemical studies have been carried out to explore this issue (Koster et al., 2005; Nagarajan et al., 2005; Shuman, 1998), and structures of the isolated domains of the *vaccinia* virus enzyme have been reported (Cheng et al., 1998; Sharma et al., 1994). Despite a wealth of biochemical and structural data, however, progress in understanding this system has been limited by lack of structural data for the poxvirus TopIB-DNA complex. In order to establish a framework for understanding the unique features of the poxvirus topoisomerase, we have determined the crystal structures of two *variola* virus topoisomerase-DNA complexes, representing the noncovalent and covalent reaction intermediates shown in Figure 1A.

Results and Discussion

Complex Design and Structure Determination

We first crystallized *variola* TopIB (vTopIB) with a 13 bp DNA duplex containing the conserved core sequence 5′-CCCTT and optimized flanking sequences (Hwang et al., 1999a). Upon cleavage of this substrate by vTopIB (Figure 1B), the trinucleotide on the 3′ side of the cleavage site was released from the complementary strand and diffused out of the active site, trapping a covalently linked topoisomerase-DNA complex (Nunes-Duby et al., 1987). An essential step in obtaining well-diffracting crystals was the substitution of two nonconserved surface cysteine residues by serine to eliminate intermolecular disulfide bond formation. As described later, this C100S, C211S mutant is nearly as active as the wild-type enzyme in plasmid relaxation assays. The structure of the covalent vTopIB-DNA complex was determined at 2.9 Å using multiwavelength anomalous scattering from selenomethionine-substituted enzyme and then refined to a final resolution of 2.7 Å. Crystallographic data are summarized in Table 1, and representative electron density is shown in Figures 1C and 1D.

Based on these results, we designed a DNA substrate to mimic the cleavage product of the 13 bp duplex,

*Correspondence: vanduyne@mail.med.upenn.edu (G.D.V.); bushman@mail.med.upenn.edu (F.D.B.)

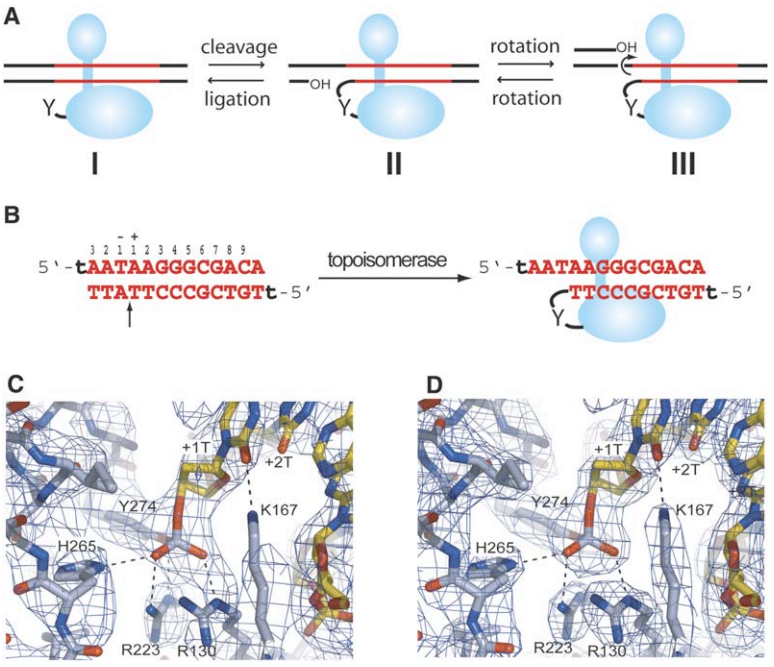

Figure 1. The Type IB Topoisomerase Reaction and Electron Density for the Covalent vTopIB-DNA Complex

(A) During the topoisomerase reaction cycle, the topoisomerase initially binds by wrapping around the substrate DNA with its two domains (intermediate I) (Cheng et al., 1998; Hwang et al., 1999b; Sekiguchi and Shuman, 1994; Shuman, 1998). If the correct DNA sequences are present, the enzyme is activated to carry out a transesterification reaction in which a conserved active site tyrosine residue attacks the phosphodiester on the 3′ side of residue +1, resulting in the formation of a covalent 3′-phosphotyrosine linkage between the enzyme and the DNA substrate (intermediate II). This permits rotation of supercoiled DNA duplexes around the site of the nick, resulting in DNA relaxation (intermediate III) (Champoux, 2001; Koster et al., 2005; Shuman, 1998; Stivers et al., 1997). The 5′-hydroxyl group liberated during the initial cleavage event then attacks the phosphotyrosine linkage to run the cleavage reaction in reverse, resealing the DNA break, and the enzyme releases from DNA to complete the reaction cycle.

(B) Formation of the covalent topoisomerase-DNA complex. The duplex DNA substrate used for complex formation and crystallization is shown, along with the numbering scheme used throughout the text and figures. Upon cleavage of the DNA substrate, the trinucleotide on the 3′ end of the cleavage site (residues −1, −2, and −3) is released, trapping the covalent enzyme-DNA complex. Note that the numbering scheme used here for poxvirus TopIB substrates differs from that used for the eukaryotic cellular topoisomerases. The enzyme attaches to the +1 nucleotide in the poxvirus TopIB convention, whereas the enzyme attaches to the −1 nucleotide in the cellular TopIB convention.

(C) Experimental electron density of the covalent vTopIB-DNA complex. The map was computed at 2.9 Å using phases from multiwavelength selenomethionine phasing and contoured at 1.2 standard deviations. The active site of the enzyme is shown, where covalent linkage between Tyr274 and the +1 phosphate is evident. Conserved catalytic residues are labelled, and important hydrogen bonds are shown.

(D) The same view as in (C), but weighted $2F_o–F_c$ electron density is shown following refinement at 2.7 Å.

where the scissile phosphate is present as an uncleavable 3′-terminal phosphate group. Crystallization of this substrate with vTopIB led to formation of a noncovalent vTopIB-DNA complex in a nearly isomorphous crystal lattice. These crystals diffracted to 1.9 Å resolution, which allowed us to clearly visualize solvent molecules in the protein/DNA interface and in the active site. The structure was refined to conventional R and R_{free} values of 0.244 and 0.197, respectively (Table 1). Electron density for the noncovalent complex is shown in Figure S1 in the Supplemental Data available with this article online. Both vTopIB-DNA complex structures have been deposited with the Protein Data Bank, with accession codes 2H7F (covalent complex) and 2H7G (noncovalent complex).

Architecture of the Topoisomerase-DNA Complex

The covalent and noncovalent smallpox vTopIB-DNA complex structures are similar throughout, with large differences present only in the active site of the enzyme (rmsd 0.90 Å, excluding residues 264–288). The topoisomerase is folded into two domains, as anticipated from previous work on related poxviruses (Cheng et al., 1998; Cheng and Shuman, 1998; Hwang et al., 1999b; Sharma et al., 1994). The two protein domains bind on either side of the core 5′-CCCTT-3′ sequence, forming a C-shaped clamp around the DNA (Figure 2A), as originally proposed based on biochemical data (Sekiguchi and Shuman, 1994). A secondary structure assignment for the full-length smallpox topoisomerase in the DNA bound structures versus those found in the isolated domains is provided in Figure S2.

The amino-terminal domain (N domain) is composed of a twisted, five-stranded antiparallel β sheet (β1–β5) with two short α helices (α1 and α2). The β5 strand of this domain is bound deeply in the major groove of the core DNA sequence, where it makes extensive direct contacts with the bases. There are very few changes in secondary or tertiary structure that occur upon DNA binding, based on comparison with the isolated N domain from *vaccinia* TopIB (Sharma et al., 1994). Superposition of the DNA bound *variola* N domain and the unbound *vaccinia* N domain results in an rmsd of 0.7 Å for Cα atoms.

The larger catalytic domain of vTopIB is centered on the opposite, minor groove face of the core DNA sequence, and the two domains are connected by the α3 helix. The long and sharply bent α3 helix forms the side of the C-shaped clamp (Figure 2A), passing along the DNA near positions +1 and +2, where the side chains of His76 and Arg80 contact the phosphate backbone (Figures 2A and 2B). Although the topoisomerase "clamp" formed around the core recognition site appears to be open on one face, a salt bridge between Lys65 in the β4–β5 hairpin and Glu139 in the α5 helix links the two domains in the noncovalent complex to fully encircle the DNA (Figure 2B). This salt bridge is not present in the covalent complex, due to an alternative choice of hydrogen bonding partners for Lys65 and Glu139. There are no significant changes in

Table 1. Summary of Crystallographic Data

	Noncovalent	Covalent (Native)	Covalent (SeMet MAD)		
Resolution	1.9 Å	2.7 Å	2.9 Å		
Space group	$C222_1$	$C222_1$	$C222_1$		
Cell constants (Å)	a = 66.2	a = 68.6	a = 68.5		
	b = 133.7	b = 137.0	b = 137.3		
	c = 113.0	c = 113.2	c = 112.8		
Wavelength (Å)	1.0332	0.97917	0.97952	0.97935	0.96394
Completeness (%)	96.2 (89.1)	99.7 (99.6)	97.5 (98.7)	97.7 (99.0)	97.7 (99.0)
R_{merge}	0.068 (0.532)	0.038 (0.285)	0.069 (0.335)	0.071 (0.347)	0.069 (0.354)
Total Reflections	422,113	312,043	311,572	323,269	315,893
Unique Reflections	36,403	14,320	11,747	11,773	11,768
I/σ	27.0 (1.57)	28.1 (8.23)	26.15 (4.88)	27.24 (4.96)	25.66 (4.73)
Redundancy	4.2 (2.1)	4.3 (4.3)	5.8 (5.9)	6.0 (6.1)	6.0 (6.1)
MAD Phasing (SOLVE)					
Z score			32.02		
Figure of merit			0.55		
Number of sites found			9		
Resolution			3.0 Å		
Refinement	Noncovalent	Covalent (Native)			
R_{free}	0.243 (0.313)	0.237 (0.370)			
R_{work}	0.197 (0.273)	0.191 (0.315)			
Number of atoms					
Protein	2629	2581			
DNA	510	509			
Water	395	54			
Average B factors ($Å^2$)					
Protein	43.03	68.98			
DNA	43.16	70.16			
Water	49.96	66.36			
Rmsd					
Bond lengths (Å)	0.014	0.011			
Bond angles (°)	1.704	1.530			

Numbers in parentheses represent values in highest-resolution shell.

backbone conformation in these regions, indicating that the covalent and noncovalent complexes do not differ by a domain-level opening or closing of the protein clamp around the DNA substrate.

In the human TopIB-DNA (hTopIB-DNA) complex, the protein forms a more substantially closed clamp around the DNA through interactions between loops arising from N-terminal subdomain I and the catalytic domain (Figure 2C). These interacting loops were originally referred to as the "Lips" of the topoisomerase (Redinbo et al., 1998; Stewart et al., 1998) and were more recently designated "Lip1" and "Lip2," respectively (Patel et al., 2006). The poxvirus enzymes do not contain sequences corresponding to the Lip1 region. As shown in Figures 2B and 2C, there is also no structural equivalent of Lip2 in the vTopIB-DNA complex. In the structure of the isolated *vaccinia* TopIB catalytic domain (Cheng et al., 1998) and in the structure of the uncomplexed *D. radiodurans* TopIB (drTopIB) (Patel et al., 2006), the residues in the region corresponding to Lip2 are disordered. As shown in Figure 2B and discussed in more detail below, the corresponding region in vTopIB folds into an α helix when bound to DNA, and this helix plays a role in specific DNA recognition.

Overall, the vTopIB catalytic domain is primarily α-helical (α4–α12) but contains a small, three-stranded β sheet (β6–β8) that is highly conserved among the type IB topoisomerases and the tyrosine recombinases (Patel et al., 2006; Redinbo et al., 1999a; Van Duyne, 2002). A large structural reorganization of this domain occurs upon DNA binding relative to the structure of the unliganded catalytic domain (Cheng et al., 1998), with an rmsd of 3.5 Å for residues 81–310 (Figure S3 and Movie S1). The conformational change can be described as a 23° rotation of the segment spanning helices α4–α7 and the β sheet (Lobe1 in Figure S3), relative to the segment that includes helices α8–α12 (Lobe2). This subdomain rotation is crucial to formation of the enzyme active site, since the catalytic tyrosine (Tyr274) is located in Lobe2 and moves by 3.6 Å (Cα atom) upon formation of the complex with DNA. The catalytic domain forms an extensive interface with the DNA substrate upstream of the cleavage site (base pairs +1 to +9), including minor groove interactions near the active site and major groove interactions involving the α5 helix (Figure 2A).

The DNA residues downstream of the cleavage site on the cleaved strand (positions −1 to −3) were lost in the process of trapping the covalent TopIB-DNA complex (Figure 1B); thus we cannot directly observe interactions that are present between the enzyme and the downstream sequence. However, the 5′ overhang in the DNA substrate produced as a result of cleavage interacts with a symmetry-related copy of itself in the crystal lattice, taking the place of the lost trinucleotide that would normally be present 3′ of the cleavage site. The enzyme makes a number of contacts with the resulting pseudocontinuous DNA duplex in this region via the

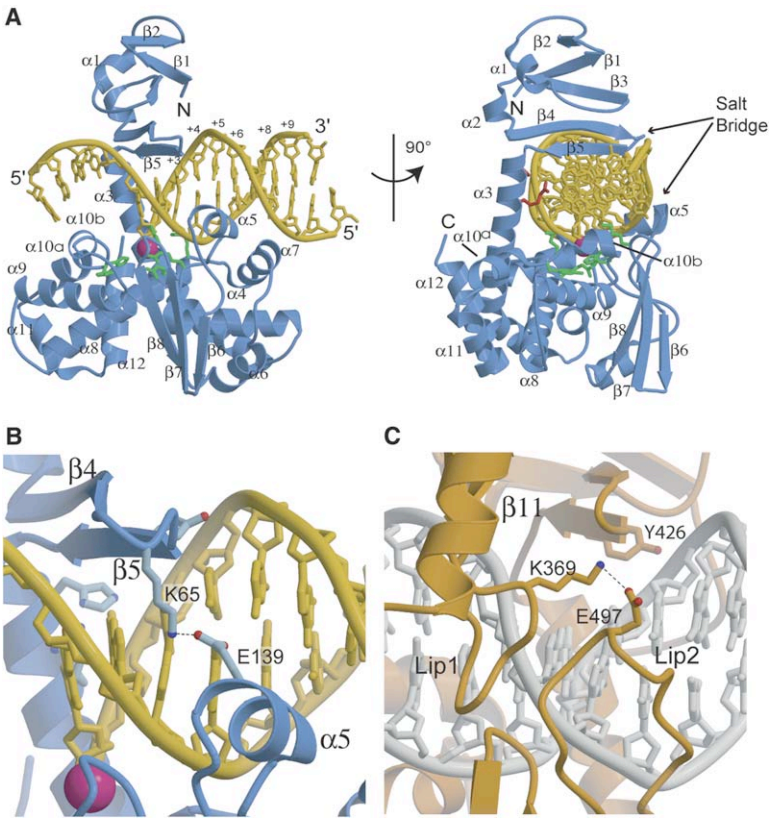

Figure 2. The *variola* Virus TopIB-DNA Complex

(A) Orthogonal views of the noncovalent protein-DNA complex. Selected secondary structure elements and the amino and carboxyl termini are indicated. The scissile phosphate (between +1 and −1 bases) is drawn as a pink sphere. Active site residues are colored green. His76 and Arg80 are colored red.

(B) Closeup of the salt bridge formed between Lys65 and Glu139 (3.2 Å) in the amino and carboxyl domains, respectively, of vTopIB in the noncovalent complex. Tyr70 from β5 and His76 from α3 are also shown.

(C) Closeup of the region in the human TopIB-DNA complex corresponding to that shown in (B). Residues Lys369 and Glu497 form a salt bridge between amino and carboxyl domains. The Lip2 region in the hTopIB-DNA complex folds into an α helix in the v-TopIB-DNA complex. There is no viral TopIB region that corresponds to the Lip1 region. Conserved Tyr426 (Tyr70 in vTopIB) is indicated.

α10a and α10b helices, strongly suggesting that the downstream DNA is contacted to at least the −2 position (data not shown). A similar conclusion was reached by modeling the DNA in the noncovalent complex as an extended DNA duplex. In the related hTopIB-DNA complex, extensive contacts are made to the downstream DNA by the coiled-coil linker (residues 636–712) and the larger N-terminal subdomains (residues 215–433), leading to a model in which these contacts control DNA rotation in the covalent intermediate (Redinbo et al., 1999a; Stewart et al., 1998). In the much smaller poxvirus enzymes, neither the coiled-coil linker nor the additional N-domain sequences are present, indicating that control of rotation in this system (Koster et al., 2005; Stivers et al., 1997) must involve a different mechanism.

Structural Basis of Sequence Specificity

The core sequence that is recognized by the poxvirus topoisomerases is 5′-(T/C)CCTT-3′, where cleavage occurs at the phosphate following the 3′-terminal thymidine (Figure 1B). In the covalent and noncovalent vTopIB/DNA crystal structures, the β5 strand in the amino-terminal domain and the α5 helix in the catalytic domain form an extensive network of major groove contacts to this core sequence (Figure 3). The side chains of residues Tyr70 and Tyr72 from β5 lie flat along the major groove, with Tyr70 covering the Cyt+3 and Cyt+4 bases and Tyr72 stacking on both the +3 ribose ring and the Thy+2 base (Figure 3A). Both tyrosine side chains also hydrogen bond to the phosphate backbone. This intimate interface explains previous observations that these residues in the *vaccinia* TopIB could be cross-linked to cytosines in the core DNA substrate (Sekiguchi and Shuman, 1996). A third direct contact from β5 involves Gln69, which makes a classic double hydrogen bonding interaction with Ade+2 (Figure 3A). Together, the major groove contacts involving the β5 strand explain the high degree of specificity for the +2 to +4 positions of the core recognition sequence.

It is interesting to note that subdomain I of human TopIB shares some similarity in structure with the N domain of poxvirus TopIB, including the placement of a β strand in the major groove of the DNA target (Redinbo et al., 1998). However, in the hTopIB-DNA complex, this β strand is shifted out of the groove by ~3 Å relative to the position observed in the vTopIB-DNA complex, thereby preventing direct contacts to the bases. With one exception, there is little sequence similarity in this region between the poxvirus and eukaryotic cellular TopIB families. Remarkably, Tyr70 is conserved in both families of enzymes, despite playing a different role in complex formation. In the hTopIB-DNA complex, the corresponding residue (Tyr426) is both shifted out of the major groove and rotated so that it interacts only with the flanking ribose and phosphate groups (Figure 2C).

The α5 helix from the vTopIB catalytic domain also forms a complex network of contacts to the major groove of the DNA substrate (Figure 3B). In this case, water molecules play a more prominent role, forming numerous bridging hydrogen bonds that are readily visualized in the high resolution noncovalent enzyme-DNA complex (data not shown). In the core recognition sequence, Tyr136 packs against the +3 sugar and hydrogen bonds to N7 of Gua+4, while Lys133 hydrogen

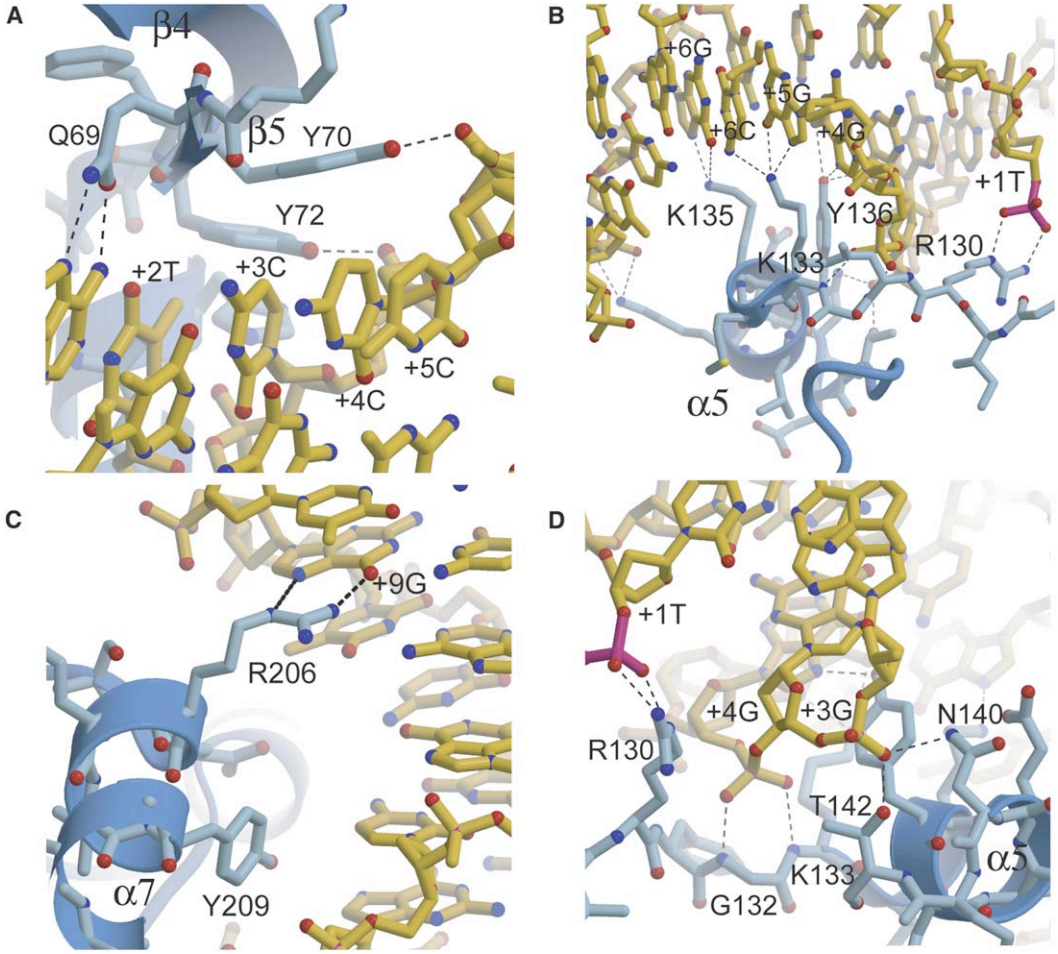

Figure 3. Specific DNA Binding and Activation of Catalysis by Smallpox Topoisomerase

(A) Specific interactions made between the β5 strand and the DNA major groove. Hydrogen bonding by Gln69, Tyr70, and Tyr72 are shown. Tyr70 and Tyr72 stack on the Cyt bases of residues +3, +4, and +5. The view is approximately the same as shown in Figure 2B.

(B) Specific interactions between the α5 helix and the DNA major groove. The view is down the α5 helical axis. The relative location of Arg130 in the active site is indicated.

(C) Interactions between α7 and the +6 to +9 residues.

(D) Close contact between the backbone amides of Gly132 and Lys133 and the +4 phosphate. This peptide segment is flanked by the α5 recognition helix and by Arg130. The view is rotated 180° relative to that shown in (B).

bonds to both the N7 and O6 atoms of guanine in position +5. In the case of Lys133, it seems likely that a minor adjustment of the side chain would allow it to interact primarily with the N7 atom of an adenine base in the +5 position, explaining the more relaxed requirement for either Thy or Cyt on the opposite strand. Outside of the core recognition sequence, Lys135 from this helix hydrogen bonds to N7 of the +6 Gua base.

The observation of helix α5 in the vTopIB-DNA complex was not expected. This region (residues 133–143) is disordered in the structures of the *vaccinia* TopIB catalytic domain and the drTopIB protein. It was logical to assume that, upon binding DNA, these residues would form an ordered loop analogous to the Lip2 segment in the human TopIB/DNA structures (Figure 2C) and that this loop would interact primarily with the sugar-phosphate backbone of the DNA (Cheng et al., 1998; Patel et al., 2006). Instead, this region of poxvirus TopIB folds into an α helix and docks in the major groove where it interacts with both the bases and the backbone. The poxvirus TopIB enzyme therefore achieves its specificity for the core recognition sequence through the N domain β5 and the C domain α5 interactions with bases in the major groove. The β5 interactions specify positions +2, +3, and +4, and the α5 interactions specify positions +4 and +5.

The sequence chosen for the region upstream of the core recognition site (positions +6 to +9) in these structural studies was based on identification of an optimal target for poxvirus topoisomerases (Hwang et al., 1999a). In addition to the Lys135 interaction discussed above, vTopIB makes direct contacts to bases in this region via Arg206 and Tyr209 in the α7 helix (Figure 3c). Arg206 makes a canonical bidentate hydrogen bonding interaction with Gua+9, representing the most upstream contact between enzyme and substrate that we observe. Tyr209 makes van der Waals contact with the +6 Cyt base. As with other specific protein-DNA complexes, there are numerous polar and nonpolar interactions between the vTopIB enzyme and the sugar-phosphate

backbone of the DNA duplex. All of the direct vTopIB/DNA interactions observed in the noncovalent complex are summarized schematically in Figure S4.

In addition to the specific interface formed by the β5 and α5 motifs discussed above, the TopIB active site may also contribute to DNA sequence specificity. The side chain of Lys167 hydrogen bonds to O2 of Thy+1 in the minor groove, an interaction that is similar to that seen in hTopIB-DNA complexes (Champoux, 2001) and in the tyrosine recombinases (Van Duyne, 2002). On the major groove face of the same +1 base pair, Arg80 from the α3 helix stacks its aromatic guanidino group on the C5-methyl groups of Thy+1 and Thy+2. Together, the Lys167 and Arg80 interactions may explain the preference for Thy in the +1 position.

The availability of several human TopIB-DNA complex structures (Redinbo et al., 1998, 1999b, 2000; Stewart et al., 1998) allows us to compare the protein DNA interfaces formed by the highly specific viral TopIB to the less-specific human enzyme. In vTopIB, there are nine residues that make direct interactions with DNA bases in the major groove (Figure S4). Some side chains make multiple independent contacts (e.g., Tyr70 and Tyr72; Figure 3A). In contrast, the hTopIB enzyme makes no direct contacts to bases in the major groove, and the binding interface is almost entirely formed between the protein and the DNA backbone. Despite the differences in specificity and sizes between the two enzymes (hTopIB is 91 kDa), the amount of solvent accessible surface area that is buried in the core protein-DNA interfaces is remarkably similar. The vTopIB-DNA complex buries ~3100 Å^2 of accessible surface in the region upstream of the cleavage site (base pairs +1 to +10). The human complex buries ~2700 Å^2 of accessible surface in the same region. In both cases, the topoisomerase proteins contact the DNA substrate downstream of the cleavage site as well, leading to a total buried surface of ~4500 Å^2 in the human TopIB/DNA interface. The corresponding interface in the vTopIB complex with an extended DNA duplex is expected to be somewhat less than this, given that the viral enzyme lacks many of the protein motifs that make downstream contacts in the human enzyme.

Structural Analysis of Poxvirus TopIB Mutants

A wealth of mutagenesis data exists for the *vaccinia* virus TopIB enzyme that can now be interpreted in the context of the specific interface observed in the *variola* TopIB-DNA complex. A partial list of reported mutations (190 mutants; 146 residues) and their effects on catalysis is given in Table S1, with corresponding literature references. We have divided these mutants into two groups: those that reduce plasmid relaxation activity by 50% or more and those that do not. In Figure 4A, these mutants are mapped onto a color-coded surface of vTopIB. Most strikingly, substitutions that have the strongest effect on topoisomerase catalysis (shown in red) map almost entirely to three distinct locations: the β5 region, the α5 region, and the active site. Since mutagenesis data are not available to aid in the interpretation of some of the protein-DNA contacts observed in the vTopIB-DNA complex, we constructed an additional set of mutants and analyzed their ability to relax negatively supercoiled DNA (Figures 4B and 4C). Also included in Figure 4B are relaxation data for vTopIB active site mutants, which show the expected levels of catalytic impairment relative to those determined for the *vaccinia* and human TopIB enzymes (the active site residues are discussed in more detail below).

In the β5 region of vTopIB (Figure 3A), mutations of Tyr70 or Tyr72 have already been shown to result in defects in DNA binding, cleavage, and relaxation (Table S1). We analyzed the Gln69Ala mutant and found that it is also defective in relaxation (Figure 4B). Thus, mutation of any of the three residues that make direct base contacts in the vTopIB β5-DNA interface leads to defects in relaxation activity. Interestingly, all three of these residues are conserved in drTopIB, suggesting that this eubacterial TopIB enzyme may share some of the core sequence preferences identified for the viral enzymes.

In the α5 region (Figure 3B), mutation of Tyr136 to Asp or Ala caused a 100-fold drop in relaxation activity, whereas mutation of the same residue to Ser resulted in wild-type activity (Table S1). Simple modeling of the Tyr136Ser mutation in the vTopIB-DNA complex suggests that Ser would be ideally positioned to hydrogen bond to the phosphate backbone, perhaps explaining why this substitution is tolerated. The Tyr136Ala mutant was found to be more defective in the cleavage step of the reaction than in ligation, leading to the conclusion that this residue may be involved in an activation step prior to cleavage (Wittschieben and Shuman, 1997). In the context of the current structure, it seems likely that Tyr136 contributes to sequence-specific activation of catalysis rather than to closure of a clamp involving a Lip-like region, as has been suggested (Patel et al., 2006). Lys133 and Lys135 in the α5 helix also make direct contacts to bases, and their mutations to alanine result in modest 3-fold and 2-fold decreases in relaxation, respectively (Figure 4B). Neither is conserved in drTopIB, and, although Lys135 is conserved in the cellular eukaryotic enzymes, it interacts with a phosphate group in the hTopIB-DNA complex.

A particularly interesting site of previous mutagenesis in this region is Leu137, which is positioned in the middle of the α5 helix. This side chain is located on the opposite face of α5 that interacts with the DNA substrate's major groove. Most residues would likely be accommodated as substitutions at this position, based on inspection of the structure. One residue that would not be expected to be tolerated in this position is proline, which would severely disrupt or distort the local α5 helical structure. Indeed, the Leu137His mutant has wild-type relaxation activity, but the Leu137Pro mutant is severely defective in relaxation, cleavage, and ligation (Wittschieben and Shuman, 1994).

Active Site Organization

The active site of vTopIB (Figures 1C and 1D and 5A–5C) contains the conserved catalytic residues Lys167, Arg130, Arg223, His265, and Tyr274, each of which has been the subject of biochemical investigation (Cheng et al., 1997; Krogh and Shuman, 2000; Nagarajan et al., 2005; Petersen and Shuman, 1997; Wittschieben and Shuman, 1997). Arg130, Arg223, and His265 form hydrogen bonds to the scissile phosphate, and Lys167 contacts the +1 base on the scissile strand (Figure 5A). A highly informative structural model for understanding

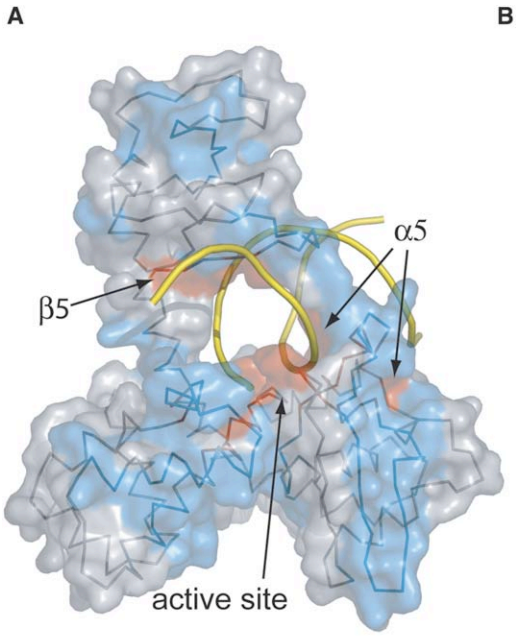

B

Enzyme	Relaxation Time (min)*
wild-type	6
C100S	6
C211S	8
CSCS §	11
CSCS Q69A	32
CSCS E124A	12
CSCS E124Q	6
CSCS R130A	>1440
CSCS K133A	30
CSCS K135A	21
CSCS K167A	>1440
CSCS D168A	700
CSCS R206A	8
CSCS Y209A	13
CSCS R223A	>1440
CSCS H265A	350
CSCS Y274F	>1440

* time to 50% conversion of starting supercoiled plasmid
§ C100S, C211S double mutant is abbreviated CSCS

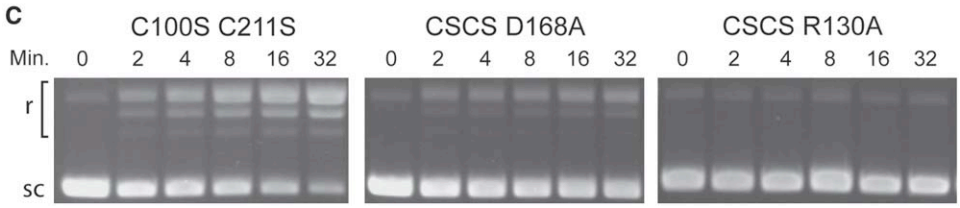

Figure 4. Structure-Function Relationship of vTopIB Mutants

(A) Mapping of the mutants from Table S1 and in (B) onto the surface of vTopIB. Mutations that cause a decrease of more than 50% in relaxation activity are colored red. Other tested mutants are colored blue. The three primary hot spots for mutagenesis are indicated.
(B) Variola TopIB mutants generated and tested for supercoiled plasmid relaxation activity based on the structures described here.
(C) Examples of plasmid relaxation time courses for three of the mutants listed in (B). sc, supercoiled; r, relaxed forms.

catalysis in the TopIB family of enzymes comes from a recently described *Leishmania donovani* TopIB (ldTopIB)-DNA-vanadate complex (Davies et al., 2006). Since vanadium can form a pentacoordinate complex with oxygen ligands and substitute for the normal phosphodiester linkage, this structure effectively mimics the expected transition state of the topoisomerase cleavage and ligation reactions. Consistent with the vanadate

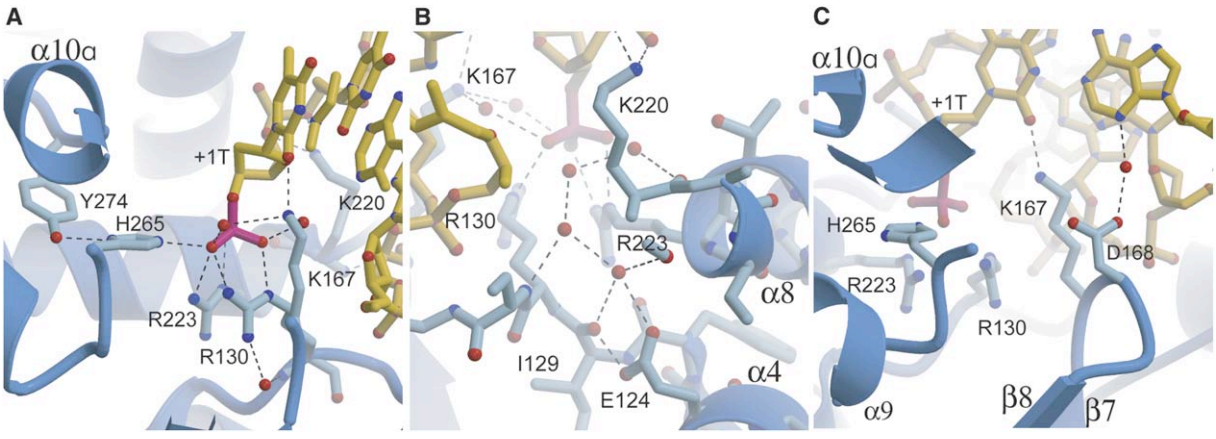

Figure 5. Active Site of the Noncovalent *variola* TopIB-DNA Complex

(A) View showing the conserved catalytic residues Arg130, Lys167, Arg223, His265, and Tyr274 as seen in the noncovalent complex.
(B) View of the active site showing the hydrogen bonding network involving Glu124. Aside from the water-mediated interaction shown, this residue is buried in the hydrophobic core of the catalytic domain.
(C) View of the active site showing the position of Asp168 relative to Lys167 and Arg130.

complex structure and with a great deal of structural and biochemical studies (Champoux, 2001; Nagarajan et al., 2005; Shuman, 1998), the prevailing model for phosphoryl transfer catalysis by this family of enzymes can be described as follows: (1) the active site is assembled (if not already preactivated) by formation of the appropriate enzyme-substrate complex; (2) Arg130, Arg223, and His265 stabilize the buildup of negative charge in the transition state as Tyr274 attacks the scissile phosphate; (3) Arg130 and Lys167 together contribute to protonation of the O5′-hydroxyl leaving group (the direct proton donor is not known); and (4) following strand rotation, the covalent 3′-phosphotyrosine intermediate formed upon expulsion of O5′ is then the target for ligation, where the cleavage reaction is run in reverse with O5′ as nucleophile and Tyr274 as the leaving group. Interestingly, no protein residue has been identified that acts as general base/acid catalyst on the Tyr274 hydroxyl group during cleavage and ligation. Instead, an active site water molecule has been suggested to play this role (Davies et al., 2006; Redinbo et al., 2000).

The vTopIB-DNA complexes described here were designed to provide high-resolution structural models of the specific enzyme-DNA interface. Both complexes lack the 5′-hydroxyl leaving group, which means that only limited new insight can be provided with respect to general acid catalysis, relative to existing structural models of TopIB and tyrosine recombinase systems. However, the covalent and noncovalent vTopIB-DNA complex structures have provided several interesting and potentially important observations with respect to the enzyme active site.

First, the most significant difference between the covalent and noncovalent topoisomerase-DNA complex structures is the positioning of the Tyr274 nucleophile (compare Figures 1C and 5A). The distance between the Tyr274 hydroxyl group and the scissile phosphate in the noncovalent complex is ~8 Å, indicating that a rather large movement of the α10a–α10b segment (Figure 2A and Figure S2) must occur during cleavage. This arrangement is quite different than that seen in comparing the covalent versus noncovalent hTopIB-DNA complexes, where the catalytic tyrosine position moves by much less (Redinbo et al., 1998).

Some of the difference in tyrosine positioning observed for the viral system may be due to the lack of downstream duplex in the vTopIB-DNA complexes, which may allow the catalytic subdomain containing Tyr274 to adopt a slightly altered position. This implies that this subdomain (residues 218–314; Lobe2 in Figure S3) must be inherently quite flexible, which is consistent with the large conformational differences observed between the unbound *vaccinia* TopIB catalytic domain (Cheng et al., 1998) and the same domain in vTopIB when bound to DNA (Figure S3 and Movie S1). Interestingly, the position of Tyr274 observed in the noncovalent vTopIB-DNA complex is intermediate between that observed in the unliganded catalytic domain and that observed in the covalent complex with DNA, suggesting that the noncovalent complex may represent a snapshot on the active site assembly pathway. The observed flexibility in the vTopIB complex is also consistent with the high degree of plasticity observed when comparing multiple structures of hTopIB-DNA complexes (Redinbo et al., 1999b).

A second surprising observation in the vTopIB-DNA complex active site is the unusual structural role of Glu124. This residue is almost entirely buried in the hydrophobic core of the catalytic domain, where one of its carboxyl oxygen atoms receives a hydrogen bond from a tightly bound water molecule located in the active site pocket (Figure 5B). The second carboxyl oxygen of this residue is 2.6 Å from the carbonyl oxygen of Ile129. This close contact requires that either the Glu124 side chain is in the neutral, protonated form or that the Ile129-Arg130 peptide bond adopts the normally disfavored imidic acid tautomer. The crystallization conditions used for the covalent and noncovalent topoisomerase-DNA complexes (pH 8) would not be expected to artificially protonate Glu124, making it unlikely that we are observing an artifact of crystallization conditions. Glu124 is conserved among the orthopox virus topoisomerases but is not conserved among the other eukaryotic type IB enzymes. Mutation of this residue to Ala or Gln has little effect on enzyme relaxation (Figure 4B), indicating that it does not play a crucial catalytic role. Further work will be required to determine why the poxviruses have maintained this unusual structural element.

A third observation involves Asp168, an active site residue that is conserved among eukaryotic TopIB enzymes. This residue forms a water-mediated interaction with N3 of the +1 Ade in the minor groove and is located adjacent to Lys167, which interacts with the +1 Thy base. The position of this residue is similar in structures of hTopI-DNA complexes (Champoux, 2001) and in the ldTopIB/DNA/vanadate transition state model (Davies et al., 2006). This residue is of interest because it is close to both Lys167 and Arg130, which have been implicated in general acid catalysis (Krogh and Shuman, 2002; Nagarajan et al., 2005). A small pocket is formed between Asp168, Lys167, and Arg130, which would be a logical place for the 5′-hydroxyl group to reside prior to the ligation step of the topoisomerase reaction cycle. Curiously, we found little biochemical data available to indicate whether Asp168 is important for catalysis. A mutant hTopIB has been isolated where both Asp533 (equivalent to poxvirus Asp168) and Asp583 were substituted by glycine (Tamura et al., 1991). This double mutant is resistant to camptothecin (discussed below) and retains ~10% activity compared to the wild-type enzyme (Yanase et al., 1999).

We found that the vTopIB Asp168Ala mutation results in a 60-fold drop in relaxation activity (Figure 4B), indicating that this residue may in fact play a catalytic role. It is interesting to note that the drTopIB enzyme has histidine in this position. Histidine, like aspartic acid, could participate directly or indirectly in acid-base catalysis. The related tyrosine recombinases do not have a conserved acidic residue or histidine in an equivalent position. Instead, serine and threonine tend to be highly represented adjacent to the catalytic lysine (Nunes-Duby et al., 1998).

Activation of Catalysis by Sequence-Specific DNA Recognition

A goal in our structural studies of vTopIB was to understand how catalysis could be coupled to sequence-specific DNA binding. The structures described here

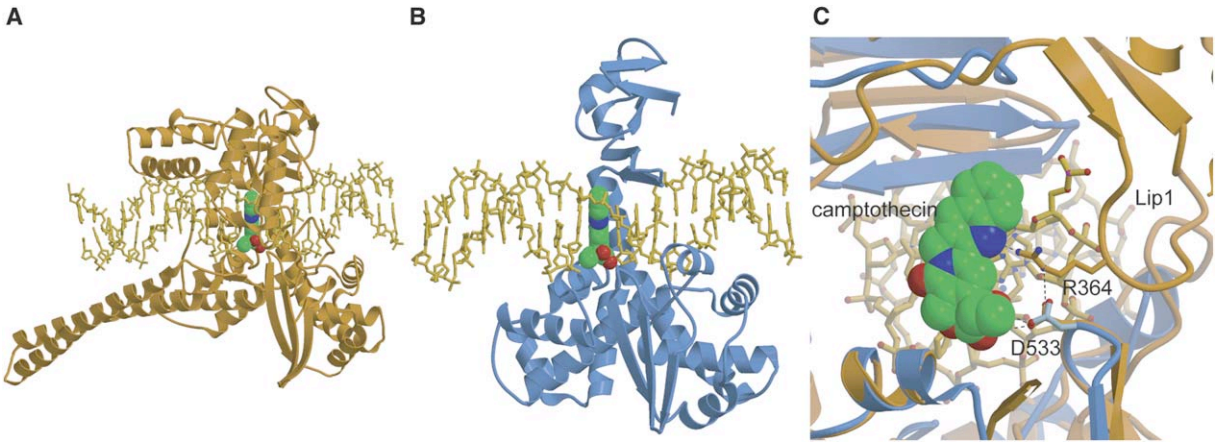

Figure 6. Drug Binding to TopIB Enzymes

(A) Structure of the hTopIB-DNA-camptothecin complex (Staker et al., 2005). The bound drug (space-filling model) is located between the +1 and −1 base pairs.

(B) Model of the vTopIB-DNA-camptothecin complex obtained by superimposing the human complex onto the covalent vTopIB-DNA complex structure. The downstream duplex DNA from the human complex was included in the model.

(C) Superposition of the structure shown in (A) with the model shown in (B), as viewed along the DNA axis (from the left), with protein and DNA downstream of the cleavage site cut away. Only the interaction involving Asp533 could be preserved in the viral complex. hTopIB is orange and vTopIB is blue.

provide a strong indication of how this is likely to occur. The segment immediately preceding α5 contains the essential active site residue Arg130. As shown in Figure 3D, specific docking of α5 into the major groove allows the preceding polypeptide chain to form a close interaction with the phosphate backbone at the +4/+5 phosphate on the noncleaved strand. Here, the amide hydrogens of Gly132 and Lys133 are able to straddle this phosphate and position Arg130 in the active site of the enzyme. In the absence of a core recognition sequence, the α5 and β5 major groove binding elements of the enzyme would not be able to form the intimate interface shown in Figures 2 and 3, and as a result it seems unlikely that Arg130 could be properly positioned to participate in catalysis.

The hTopIB enzyme, which has a much lower level of sequence specificity, uses an alternative mechanism to position this catalytic arginine residue. Human TopIb has a loop (Lip2; Figure 2D) in place of the poxvirus helix α5 that contacts only the phosphate backbone of the DNA substrate (Redinbo et al., 1998; Stewart et al., 1998). A similar set of peptide backbone amide-phosphate contacts are formed adjacent to the catalytic Arg488 (equivalent of poxvirus Arg130) in this system, but in this case nonspecific contacts in the flanking loop cooperate to build this portion of the enzyme's active site. In poxvirus TopIB, docking of α5 in the adjacent major groove appears to be required for assembly of an active enzyme. This idea is consistent with earlier proposals that Tyr136 (Figure 3b) is involved in an activation step prior to cleavage (Wittschieben and Shuman, 1997).

Antiviral Compounds that Target TopIB Enzymes

In addition to providing insight into the unique mechanistic features of the orthopox virus topoisomerases, the structures of the vTopIB-DNA complexes described here represent an obvious target for antiviral drugs against poxvirus infections. Several classes of DNA intercalating compounds that target hTopIB are currently in use as anticancer and anti-infective agents. These drugs act as cellular poisons by binding to and trapping the covalent topoisomerase-DNA complex that forms transiently during the reaction, effectively turning the enzyme into an agent that stabilizes toxic DNA breaks in the genome. The crystal structures of covalent hTopIB-DNA complexes bound by intercalating agents from several classes demonstrate that the drugs bind between the +1 and −1 base pairs of the DNA substrate and prevent religation by distancing the scissile phosphate from the 5′-hydroxyl of the −1 base (Staker et al., 2005; Staker et al., 2002).

The pharmacological properties of hTopIB and vTopIB are in general quite different (Shuman et al., 1988). For example, the hallmark hTopIB poison camptothecin has little effect on poxvirus TopIB enzyme at moderate concentrations. The vTopIB-DNA complex structures provide a plausible explanation of why camptothecin is ineffective against the viral target. A comparison of the hTopIB/DNA/camptothecin structure to a model of the corresponding vTopIB complex is shown in Figures 6A and 6B. The most striking difference between the complexes is the extent to which the drug is encapsulated by the much larger human enzyme. The extended N-terminal subdomains in hTopIB form a large flap that covers much of the intercalation site, whereas the vTopIB enzyme has no corresponding structural elements and the modeled drug is largely solvent exposed in this region.

A closeup of the two superimposed structures (Figure 6C) also reveals that the vTopIB enzyme cannot make many of the interactions to the bound drug that are observed in the human enzyme complex. Asp533 and Arg364 form a hydrogen bond network between themselves and camptothecin in the human TopIB complex. Although Asp533 is conserved in the poxvirus enzymes

(the corresponding vTopIB residue is Asp168, discussed previously), there is no equivalent of Arg364. Indeed, the entire Lip1 region (Figure 6C, Figures 2B and 2C) is absent in the poxvirus enzymes. This region is important for sensitivity to camptothecin, since mutations in Lip1 are known to confer resistance to the drug (Chrencik et al., 2004). The comparisons shown in Figure 6 not only suggest why camptothecin is ineffective as a viral TopIB poison, but they also illustrate a likely reason why identification of alternative agents that act via the same mechanism against poxvirus TopIB has been so difficult. The minimal nature of the viral enzyme leaves few opportunities for drug-stabilizing interactions that are presumably necessary to trap and accumulate the covalent intermediate of the reaction.

Several compounds have been recently identified that are, in fact, potent inhibitors of the *vaccinia* TopIB enzyme's ability to relax negatively supercoiled DNA, some with IC_{50} values in the nM range (Bond et al., 2006). Although these compounds do not accumulate the covalent intermediate, some appear to specifically target the enzyme-substrate complex after cleavage has occurred. In principle, it may be possible to modify such compounds that bind with high affinity to the covalent complex so that they inhibit the ligation reaction in addition to inhibiting relaxation. Since the TopIB enzyme is not strictly required for poxvirus replication (Moss, 2001), inhibition of the enzyme may alone be insufficient to arrest viral infection and growth. Targeting of the covalent enzyme-DNA intermediate, as occurs with hTopIB poisons, would appear to be a better strategy. A three-dimensional structure of the inhibitors in question bound to the covalent vTopIB-DNA complex would be an ideal platform for such studies and will be a focus of further work in this area.

Experimental Procedures

Topoisomerase and DNA Preparations

We first generated an expression construct encoding the *variola* virus topoisomerase by site-directed mutagenesis of the *vaccinia* virus gene (the *vaccinia* WR topoisomerase differs from that of *variola* major by three amino acid changes: D24N, E47G, and E159K). The smallpox enzyme was later modified to reduce intermolecular disulfide formation by changing both cysteine residues (C100 and C211) to serine. *Variola* TopIB was overexpressed in *E. coli* BL21(DE3) cells and purified to homogeneity by ion exchange chromatography on SP Sepharose (Pharmacia) and Uno-S (BioRad) columns, followed by size exclusion chromatography on Sephadex S-75 (Pharmacia). The protein was concentrated in 20 mM sodium HEPES (pH 7.5) and 400 mM NaCl and stored at 4°C. Selenomethionine-substituted protein was overexpressed using the methionine auxotroph B834(DE3) grown in EZ Rich methionine-free medium (Teknova) supplemented with 100 mg/L D/L-selenomethionine and purified in the same manner.

Oligonucleotides were synthesized by the Keck Biotechnology Facility at Yale University and were purified by anion ion exchange chromatography at pH 12 on a DNA-Pac column (Dionex) followed by concentration on SepPak (Waters) cartridges and buffer exchange/concentration in Centricon-3 devices (Millipore). Oligonucleotides were annealed in 20 mM sodium HEPES (pH 7.5), 400 mM NaCl.

Crystallization and Structure Determination

Protein and DNA substrates were mixed in a 1:1.5 stoichiometry, buffer exchanged into 20 mM sodium HEPES (pH 7.5), 100 mM NaCl, and incubated at 4°C for a minimum of 18 hr prior to crystallization. Crystals were grown by hanging drop vapor diffusion where initial drops containing 127 μM topoisomerase, 200 μM DNA, and 4% polyethylene glycol (PEG) 8000, 25 mM Tris-HCl (pH 7.4), 10 mM HEPES, 50 mM NaCl were equilibrated against reservoirs containing 8% PEG 8000 and 50 mM Tris-HCl (pH 7.4). Prior to data collection, crystals were cryoprotected by transfer to 8% PEG 8000, 50 mM Tris-HCl (pH 7.4), 25% 2-methyl-2,4-pentanediol.

Diffraction data were measured at the Advanced Light Source beamlines 8.2.1 and 8.2.2. Multiwavelength data were measured at three wavelengths and processed using the HKL suite (Otwinowski and Minor, 1997). The program SOLVE (Terwilliger and Berendzen, 1999) was used to locate Se sites and phase multiwavelength data for the covalent intermediate complex at 2.9 Å. The uncleaved topoisomerase-DNA complex is nearly isomorphous to the covalent intermediate complex, and initial phases were readily determined from rigid body refinement of the covalent complex protein domains and DNA duplex.

Both structures were initially refined using CNS (Brunger et al., 1998). After addition of solvent molecules, REFMAC (Murshudov et al., 1997) was used to perform TLS refinement (Winn et al., 2001). Model building was performed with the program O (Jones et al., 1991). Parts of Figures 1–6 were made with MOLSCRIPT (Kraulis, 1991), RASTER3D (Merritt and Murphy, 1994), and PYMOL (DeLano, 2002).

Construction of Mutants and DNA Relaxation Assays

Mutants of vTopIB shown in Figure 4 were generated in the C100S, C211S background using the QuikChange (Stratagene) procedure, and the modified proteins were purified as described above for the double cysteine mutant. To assay for relaxation activity, reaction mixtures containing (per 20 μl) 50 mM Tris-HCl (pH 8.0), 0.15 M NaCl, 5% glycerol, 1 μg pUC19 plasmid DNA and 3.1 ng of topoisomerase were incubated at 25°C. Aliquots (20 μl) were removed at various times and quenched by the addition of a solution containing glycerol, bromophenol blue, and SDS (3% final concentration). Samples were analyzed by electrophoresis through 0.8% agarose gel in TAE buffer. After staining for 15 min in 0.5 μg/ml ethidium bromide, the gel was soaked for 30 min in water, photographed, and quantified using a Storm PhosphorImager (Molecular Dynamics).

Supplemental Data

Supplemental Data include four figures, one table, one movie, and Supplemental References and can be found with this article online at http://www.molecule.org/cgi/content/full/23/3/343/DC1/.

Acknowledgments

We thank Kushol Gupta, Peng Yuan, and beamline staff at ALS 8.2.1 and 8.2.2 for assistance with synchrotron data collection. This work was supported by NIH NIAID Middle Atlantic Regional Center of Excellence Grant U54 AI057168 (to F.D.B.). G.D.V. is an Investigator of the Howard Hughes Medical Institute. The Advanced Light Source is supported by the Director, Office of Science, Office of Basic Energy Sciences, of the U.S. Department of Energy under Contract No. DE-AC02-05CH11231.

Received: February 3, 2006
Revised: May 2, 2006
Accepted: June 12, 2006
Published: August 3, 2006

References

Been, M.O., Burgess, R.R., and Champoux, J.J. (1984). Nucleotide sequence preferences at rat liver and wheat germ type 1 DNA topoisomerase breakage sites in duplex SV40 DNA. Nucleic Acids Res. *12*, 3097–3114.

Bond, A., Reichert, Z., and Stivers, J.T. (2006). Novel and specific inhibitors of a poxvirus type I topoisomerase. Mol. Pharmacol. *69*, 547–557.

Brunger, A.T., Adams, P.D., Clore, G.M., DeLano, W.L., Gros, P., Gross-Kunstleve, R.W., Jiang, J.S., Kuszewski, J., Nilges, M., Pannu, N.S., et al. (1998). Crystallography & NMR system: a new

software suite for macromolecular structure determination. Acta Crystallogr. D. Biol. Crystallogr *54*, 905–921.

Champoux, J.J. (2001). DNA topoisomerases: structure, function, and mechanism. Annu. Rev. Biochem. *70*, 369–413.

Cheng, C., and Shuman, S. (1998). A catalytic domain of eukaryotic DNA topoisomerase I. J. Biol. Chem. *273*, 11589–11595.

Cheng, C., Wang, L.K., Sekiguchi, J., and Shuman, S. (1997). Mutational analysis of 39 residues of vaccinia DNA topoisomerase identifies Lys-220, Arg-223, and Asn-228 as important for covalent catalysis. J. Biol. Chem. *272*, 8263–8269.

Cheng, C., Kussie, P., Pavletich, N., and Shuman, S. (1998). Conservation of structure and mechanism between eukaryotic topoisomerase I and site-specific recombinases. Cell *92*, 841–850.

Chrencik, J.E., Staker, B.L., Burgin, A.B., Pourquier, P., Pommier, Y., Stewart, L., and Redinbo, M.R. (2004). Mechanisms of camptothecin resistance by human topoisomerase I mutations. J. Mol. Biol. *339*, 773–784.

Da Fonseca, F., and Moss, B. (2003). Poxvirus DNA topoisomerase knockout mutant exhibits decreased infectivity associated with reduced early transcription. Proc. Natl. Acad. Sci. USA *100*, 11291–11296.

Davies, D.R., Mushtaq, A., Interthal, H., Champoux, J.J., and Hol, W.G. (2006). The structure of the transition state of the heterodimeric topoisomerase I of Leishmania donovani as a vanadate complex with nicked DNA. J. Mol. Biol. *357*, 1202–1210.

DeLano, W.L. (2002). The PyMOL User's Manual (San Carlos, CA: DeLano Scientific).

Harrison, S.C., Alberts, B., Ehrenfeld, E., Enquist, L., Fineberg, H., McKnight, S.L., Moss, B., O'Donnell, M., Ploegh, H., Schmid, S.L., et al. (2004). Discovery of antivirals against smallpox. Proc. Natl. Acad. Sci. USA *101*, 11178–11192.

Hwang, Y., Wang, B., and Bushman, F.D. (1998). Molluscum contagiosum virus topoisomerase: purification, activities and response to inhibitors. J. Virol. *72*, 3401–3406.

Hwang, Y., Burgin, A., and Bushman, F.D. (1999a). DNA contacts stimulate catalysis by a poxvirus topoisomerase. J. Biol. Chem. *274*, 9160–9168.

Hwang, Y., Park, M., Fischer, W.H., and Bushman, F. (1999b). Domain structure of the type-1B topoisomerase encoded by molluscum contagiosum virus. Virology *262*, 479–491.

Jones, T., Zou, J.-Y., Cowan, S., and Kjeldgaard, M. (1991). Improved methods for building protein models in electron density maps and the location of errors in these models. Acta Crystallogr. *47*, 110–119.

Koster, D.A., Croquette, V., Dekker, C., Shuman, S., and Dekker, N.H. (2005). Friction and torque govern the relaxation of DNA supercoils by eukaryotic topoisomerase IB. Nature *434*, 671–674.

Kraulis, P.J. (1991). MOLSCRIPT: a program to produce both detailed and schematic plots of protein structures. J. Appl. Crystallogr. *24*, 946–950.

Krogh, B.O., and Shuman, S. (2000). Catalytic mechanism of DNA topoisomerase IB. Mol. Cell *5*, 1035–1041.

Krogh, B.O., and Shuman, S. (2002). Proton relay mechanism of general acid catalysis by DNA topoisomerase IB. J. Biol. Chem. *277*, 5711–5714.

Merritt, E.A., and Murphy, M.E. (1994). Raster3D Version 2.0. A program for photorealistic molecular graphics. Acta Crystallogr. D. Biol. Crystallogr. *50*, 869–873.

Moss, B. (2001). Poxviridae: the viruses and their replication. In Virology, B.N. Fields, ed. (Philadelphia: Lippincott-Raven), pp. 2637–2672.

Murshudov, G.N., Vagin, A.A., and Dodson, E.J. (1997). Refinement of macromolecular structures by the maximum-likelihood method. Acta Crystallogr. D Biol. Crystallogr. *53*, 240–255.

Nagarajan, R., Kwon, K., Nawrot, B., Stec, W.J., and Stivers, J.T. (2005). Catalytic phosphoryl interactions of topoisomerase IB. Biochemistry *44*, 11476–11485.

Nunes-Duby, S.E., Matsumoto, L., and Landy, A. (1987). Site-specific recombination intermediates trapped with suicide substrates. Cell *50*, 779–788.

Nunes-Duby, S.E., Kwon, H.J., Tirumalai, R.S., Ellenberger, T., and Landy, A. (1998). Similarities and differences among 105 members of the Int family of site-specific recombinases. Nucleic Acids Res. *26*, 391–406.

Otwinowski, Z., and Minor, W. (1997). Processing of X-ray diffraction data collected in oscillation mode. Methods Enzymol. *276*, 307–326.

Patel, A., Shuman, S., and Mondragon, A. (2006). Crystal structure of bacterial type IB DNA topoisomerase reveals a preassembled active site in the absence of DNA. J. Biol. Chem. *281*, 6030–6037.

Petersen, B.O., and Shuman, S. (1997). Histidine 265 is important for covalent catalysis by vaccinia topoisomerase and is conserved in all eukaryotic type I enzymes. J. Biol. Chem. *272*, 3891–3896.

Redinbo, M.R., Stewart, L., Kuhn, P., Champoux, J.J., and Hol, W.G.J. (1998). Crystal structures of human topoisomerase I in covalent and noncovalent complexes with DNA. Science *279*, 1504–1513.

Redinbo, M.R., Champoux, J.J., and Hol, W.G. (1999a). Structural insights into the function of type IB topoisomerases. Curr. Opin. Struct. Biol. *9*, 29–36.

Redinbo, M.R., Stewart, L., Champoux, J.J., and Hol, W.G. (1999b). Structural flexibility in human topoisomerase I revealed in multiple non-isomorphous crystal structures. J. Mol. Biol. *292*, 685–696.

Redinbo, M.R., Champoux, J.J., and Hol, W.G. (2000). Novel insights into catalytic mechanism from a crystal structure of human topoisomerase I in complex with DNA. Biochemistry *39*, 6832–6840.

Sekiguchi, J., and Shuman, S. (1994). Vaccinia topoisomerase binds circumferentially to DNA. J. Biol. Chem. *269*, 31731–31734.

Sekiguchi, J., and Shuman, S. (1996). Identification of contacts between topoisomerase I and its target DNA by site-specific photocrosslinking. EMBO J. *15*, 3448–3457.

Sharma, A., Hanai, R., and Mondragon, A. (1994). Crystal structure of the amino-terminal fragment of vaccinia virus DNA topoisomerase I at 1.6 A resolution. Structure *2*, 767–777.

Shuman, S. (1998). Vaccinia virus DNA topoisomerase: a model eukaryotic type IB enzyme. Biochim. Biophys. Acta *1400*, 321–339.

Shuman, S., and Prescott, J. (1990). Specific DNA cleavage and binding by vaccinia virus DNA topoisomerase I. J. Biol. Chem. *265*, 17826–17836.

Shuman, S., Golder, M., and Moss, B. (1988). Characterization of vaccinia virus DNA topoisomerase I expressed in Escherichia coli. J. Biol. Chem. *263*, 16401–16407.

Staker, B.L., Hjerrild, K., Feese, M.D., Behnke, C.A., Burgin, A.B., Jr., and Stewart, L. (2002). The mechanism of topoisomerase I poisoning by a camptothecin analog. Proc. Natl. Acad. Sci. USA *99*, 15387–15392.

Staker, B.L., Feese, M.D., Cushman, M., Pommier, Y., Zembower, D., Stewart, L., and Burgin, A.B. (2005). Structures of three classes of anticancer agents bound to the human topoisomerase I-DNA covalent complex. J. Med. Chem. *48*, 2336–2345.

Stewart, L., Redinbo, M.R., Qiu, X., Hol, W.G.J., and Champoux, J.J. (1998). A model for the mechanism of human topoisomerase I. Science *179*, 1534–1541.

Stivers, J.T., Harris, T.K., and Mildvan, A. (1997). Vaccinia DNA topoisomerase I: evidence supporting a free rotation mechanism for DNA supercoil relaxation. Biochemistry *36*, 5212–5222.

Tamura, H., Kohchi, C., Yamada, R., Ikeda, T., Koiwai, O., Patterson, E., Keene, J.D., Okada, K., Kjeldsen, E., Nishikawa, K., et al. (1991). Molecular cloning of a cDNA of a camptothecin-resistant human DNA topoisomerase I and identification of mutation sites. Nucleic Acids Res. *19*, 69–75.

Terwilliger, T.C., and Berendzen, J. (1999). Automated MAD and MIR structure solution. Acta Crystallogr. D. Biol. Crystallogr. *55*, 849–861.

Tian, L., Claeboe, C.D., Hecht, S.M., and Shuman, S. (2004). Remote phosphate contacts trigger assembly of the active site of DNA topoisomerase IB. Structure (Camb.) *12*, 31–40.

Van Duyne, G.D. (2002). A structural view of tyrosine recombinase site-specific recombination. In Mobile DNA II, N.L. Craig, R. Craigie,

M. Gellert and A.M. Lambowitz, eds. (Washington, D.C.: ASM Press), pp. 93–117.

Wang, J.C. (1996). DNA topoisomerases. Annu. Rev. Biochem. *65*, 635–692.

Winn, M.D., Isupov, M.N., and Murshudov, G.N. (2001). Use of TLS parameters to model anisotropic displacements in macromolecular refinement. Acta Crystallogr. D Biol. Crystallogr. *57*, 122–133.

Wittschieben, J., and Shuman, S. (1994). Mutational analysis of vaccinia DNA topoisomerase defines amino acid residues essential for covalent catalysis. J. Biol. Chem. *269*, 29978–29983.

Wittschieben, J., and Shuman, S. (1997). Mechanism of DNA transesterification by vaccinia topoisomerase: catalytic contributions of essential residues Arg-130, Gly-132, Tyr-136 and Lys-167. Nucleic Acids Res. *25*, 3001–3008.

Yanase, K., Sugimoto, Y., Andoh, T., and Tsuruo, T. (1999). Retroviral expression of a mutant (Gly-533) human DNA topoisomerase I cDNA confers a dominant form of camptothecin resistance. Int. J. Cancer *81*, 134–140.

Accession Numbers

The covalent and noncovalent TopIB-DNA complex coordinates have been deposited in the Protein Data Bank under ID codes 2H7F and 2H7G, respectively.